

Fast estimation for range identification in the presence of unknown motion parameters

LILI MA*

*Department of Electronics and Mechanical, Wentworth Institute of Technology,
Boston, MA 02115, USA*

*Corresponding author: mal@wit.edu

CHENGYU CAO

Department of Mechanical Engineering, University of Connecticut, Storrs, CT 06269, USA

NAIRA HOVAKIMYAN

*Department of Mechanical Science and Engineering, University of Illinois at
Urbana-Champaign, Champaign, IL 61801, USA*

CRAIG WOOLSEY

Department of Aerospace and Ocean Engineering, Virginia Tech, Blacksburg, VA 24061, USA

AND

WARREN E. DIXON

*Department of Mechanical and Aerospace Engineering, University of Florida,
Gainesville, FL 32611, USA*

[Received on 14 March 2008; revised on 1 February 2010; accepted on 2 February 2010]

A fast estimator is proposed and applied to the problem of range identification in the presence of unknown motion parameters. Assuming a rigid-body motion with unknown constant rotational parameters but known translational parameters, estimation of the unknown parameters is achieved by a fast estimator, followed by recursive least square extraction. The results are also extended to the case of an affine motion. Simulations demonstrate the superior performance of fast estimation in comparison to an identifier-based observer.

Keywords: range identification; fast estimator; rigid-body motion; affine motion.

1. Introduction

A variety of 3D motion estimation algorithms have been developed since 1970s, inspired by such disparate applications as robot navigation, medical imaging and video conferencing. Even though motion estimation from imagery is not a new topic, continual improvements in digital imaging, computer processing capabilities and non-linear estimation theory have helped to keep the topic current. Existing methods for 3D motion estimation include non-linear optimization formulation (Cho *et al.*, 2001; Diamantaras *et al.*, 1998; Diamantaras & Strintzis, 1996), linear least square algorithms (Papadimitriou *et al.*, 2000), extended Kalman filter (EKF; Chiuso *et al.*, 2002; Kano *et al.*, 2001; Soatto *et al.*, 1996; Azarbayejani & Pentland, 1995; Matthies *et al.*, 1989) and perspective non-linear observers

(Jankovic & Ghosh, 1995; Chen & Kano, 2002, 2004; Dixon *et al.*, 2003; Ma *et al.*, 2005b; Karagiannis & Astolfi 2005; Dahl *et al.*, 2005). Perspective non-linear observers are a class of observers that arise from a control point of view in the perspective dynamic systems framework. In general, a perspective dynamic system is a linear system whose output is observed up to a homogeneous line (Chen & Kano, 2002; Takahashi & Ghosh, 2002; Ghosh & Martin, 2002; Ghosh & Loucks, 1995; Ghosh *et al.*, 1994).

Among the aforementioned algorithms, the non-linear optimization formulation generally suffers from the initial value selection problem. The shortcoming of (total) least square algorithms, which are singular value decomposition-based, is sensitivity to noise (Diamantaras & Stintzis, 1996). Assuming that the moving object follows certain motion dynamics, an EKF can be used to estimate the motion parameters and positions. The EKF is a recursive approach that usually requires less computation time for each new set of data (e.g. each new image). State estimates are computed based on all past data and can readily extrapolate the state estimates ahead in time to aid in preprocessing the next set of data. We note that the EKF is based on the linearization about an estimated trajectory. However, for the vision-based motion estimation problem, the geometric structure of a perspective system will be lost if a linearization-based approach is taken. Efforts have been made towards other non-linear observers for perspective dynamic systems that arise in visual tracking problems. This class of non-linear observers is referred to as perspective non-linear observers.

Perspective non-linear observers are used quite often for determining the unknown states (i.e. the Euclidean coordinates) of a moving object with known motion parameters. For example, an identifier-based observer (IBO) is proposed in Jankovic & Ghosh (1995) to estimate a stationary point's 3D position using a moving camera. Another discontinuous observer, motivated by sliding mode and adaptive methods, is developed in Chen & Kano (2002) that renders the state observation error uniformly ultimately bounded. A state estimation algorithm with a single homogeneous observation (i.e. a single image coordinate) is presented in Ma *et al.* (2005b). A reduced-order non-linear observer is described in Karagiannis & Astolfi (2005) to provide asymptotic range estimates. The observers described above are based on a conventional planar imaging surface. In Ma *et al.* (2005a) and Gupta *et al.* (2006), the state estimation problem is discussed for a parabolic projection surface. All these results are based on the assumption that the motion parameters are known with the objective of estimating the unknown depth.

In this paper, we consider the case in which some of the motion parameters (the rotational parameters) are unknown constants. The objective is to estimate the 3D position along with the unknown parameters. A fast estimation scheme is applied for the estimation task. The fast estimator is further augmented with a recursive least square (RLS) algorithm to estimate the unknown parameters. Under certain persistent excitation (PE)-type conditions, the RLS algorithm ensures the convergence of parameter estimation. Preliminary results were presented in Ma (2007b).

One model for the relative motion of a point in the camera's field of view is the following linear system (Jankovic & Ghosh, 1995; Chen & Kano, 2004, 2002; Dixon *et al.*, 2003; Karagiannis & Astolfi, 2005):

$$\begin{bmatrix} \dot{X}(t) \\ \dot{Y}(t) \\ \dot{Z}(t) \end{bmatrix} = \begin{bmatrix} 0 & \omega_1 & \omega_2 \\ -\omega_1 & 0 & \omega_3 \\ -\omega_2 & -\omega_3 & 0 \end{bmatrix} \begin{bmatrix} X(t) \\ Y(t) \\ Z(t) \end{bmatrix} + \begin{bmatrix} b_1(t) \\ b_2(t) \\ b_3(t) \end{bmatrix}, \quad (1.1)$$

where the matrix $[\omega_i]$ presents the rotational dynamics, the vector $[b_i]$ corresponds to the translational motion and $[X(t), Y(t), Z(t)]^\top$ denote the coordinates of the point in the camera frame at time

instance t . Some other variables used throughout this paper is listed in Table 1. Using a conventional camera, the homogeneous output observations are

$$x_1(t) = X(t)/Z(t), \quad x_2(t) = Y(t)/Z(t). \quad (1.2)$$

The coordinate $Z(t)$ denotes the depth from the image plane to the object feature along the optical axis. It is assumed that $Z(t) > 0$ for possible motion estimation. The assumption $Z > 0$ is a reasonable assumption referring to the physical system (Chen & Kano, 2004). In general, the parameters ω_i can be time-varying functions, but in this paper we assume that $[\omega_i]$ is a constant matrix.

Figure 1 illustrates one scenario of constant $[\omega_i]$, where an omnidirectional robot is moving with constant angular velocity on a plane described by its normal vector $\vec{n} = [n_1, n_2, n_3]^T$. The motion dynamics of a feature point on the robot can be modelled by (1.1).

Let

$$[x_1(t), x_2(t), x_3(t)]^T = [X(t)/Z(t), Y(t)/Z(t), 1/Z(t)]^T. \quad (1.3)$$

The system (1.1) with output observations (1.3) is equivalent to the following system (Jankovic & Ghosh, 1995; Chen & Kano, 2002; Dixon *et al.*, 2003):

$$\left\{ \begin{array}{l} \begin{bmatrix} \dot{x}_1(t) \\ \dot{x}_2(t) \end{bmatrix} = \begin{bmatrix} b_1(t) - b_3(t)x_1(t) \\ b_2(t) - b_3(t)x_2(t) \end{bmatrix} x_3(t) \\ \quad + \begin{bmatrix} \omega_2 + \omega_1 x_2(t) + \omega_2 x_1^2(t) + \omega_3 x_1(t)x_2(t) \\ \omega_3 - \omega_1 x_1(t) + \omega_2 x_1(t)x_2(t) + \omega_3 x_2^2(t) \end{bmatrix}, \\ \dot{x}_3(t) = (\omega_2 x_1(t) + \omega_3 x_2(t))x_3(t) - b_3(t)x_3^2(t), \end{array} \right. \quad (1.4)$$

with the output

$$y(t) = [x_1(t), x_2(t)]^T. \quad (1.5)$$

Estimation of $x_3(t)$ from the visual measurements $(x_1(t), x_2(t))$ constitutes the range identification problem. Jankovic & Ghosh (1995), Chen & Kano (2002, 2004), Dixon *et al.* (2003), Ma *et al.* (2005b)

TABLE 1 *Description of variables*

Variable	Description
$[X(t), Y(t), Z(t)]^T$	Coordinates of a feature point in the camera frame at time instance t
$[x_1(t), x_2(t), x_3(t)]^T$	$[X(t), Y(t), 1]^T / Z(t)$
$\theta = [\omega_1, \omega_2, \omega_3]^T$	$(\omega_1, \omega_2, \omega_3)$ denote the skew-symmetric matrix in (1.1)
$\omega(t)$	The time-varying signal to be estimated via fast estimator
$\omega_r(t)$	An intermediate signal introduced to facilitate analysis
$\omega_e(t)$	Estimate of $\omega(t)$ via fast estimator
Γ_c	Update gain used in the fast estimator
$C(s)$	$C(s) = \frac{c}{s+c}$, a low-pass filter used in the fast estimator

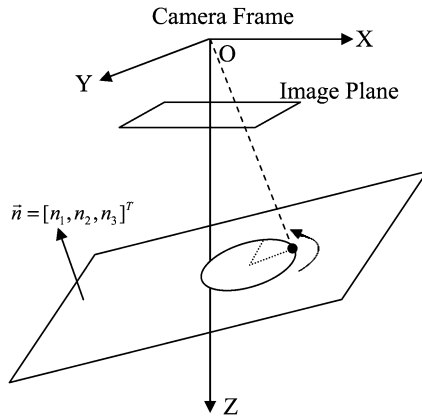


FIG. 1. Illustration of constant angular velocity where the black dot traces a path on the plane defined by \vec{n} at some frequency.

and Karagiannis & Astolfi (2005) have solved this problem assuming that the motion parameters ω_i and $b_i(t)$ in (1.1) are known (for $i \in \{1, 2, 3\}$). Here, we assume that the parameters ω_i are unknown constants. The objective is to estimate $x_3(t)$ as well as the unknown parameters ω_i . This problem can be formulated in a way that existing observers, such as those developed in Jankovic & Ghosh (1995), Chen & Kano (2002, 2004), Dixon *et al.* (2003), Ma *et al.* (2005b) and Karagiannis & Astolfi (2005), can be applied. Under certain PE-type assumptions, the approach provides an exponential convergence of both the range and the parameter estimates (Jankovic & Ghosh, 1995; Narendra & Annaswamy, 2005; Wittenmark, 1995). A more general case of the problem consists of a 3×3 rotational matrix instead of the skew-symmetric matrix as in (1.1) (Dixon *et al.*, 2003; Ma *et al.*, 2007a).

The contribution of this paper includes two aspects. One is to present a fast estimator with detailed proofs. The analysis of the fast estimator is further extended to characterize the performance of the fast estimator with respect to non-zero initialization error. The other is to discuss range identification in the presence of unknown constant rotational parameters via the fast estimator. Performance comparison of the fast estimator with the IBO is provided. The IBO has been compared with the EKF-based method in Jankovic & Ghosh (1995) to achieve comparable performance with the advantage of providing rigorous proof.

The paper is organized as follows. Range identification in the presence of unknown motion parameters via the IBO is described in Section 2. A fast estimator is presented in Section 3. Range identification via the fast estimator is described in Section 4. Section 5 provides the simulation results. Section 6 extends the analysis to general affine motion. Finally, Section 7 concludes the paper.

2. Range identification via IBO

Consider the estimation problem for the perspective dynamic system (1.4), where the motion parameters ω_i (for $i = 1, 2, 3$) are assumed to be unknown constants. Let θ be a vector of these unknown constants defined as

$$\theta = [\omega_1, \omega_2, \omega_3]^T. \quad (2.1)$$

The system (1.4) can be rewritten as

$$\begin{cases} \begin{bmatrix} \dot{x}_1(t) \\ \dot{x}_2(t) \end{bmatrix} = w_s^\top(x_1(t), x_2(t)) \begin{bmatrix} x_3(t) \\ \boldsymbol{\theta} \end{bmatrix}, \\ \begin{bmatrix} \dot{x}_3(t) \\ \dot{\boldsymbol{\theta}} \end{bmatrix} = \begin{bmatrix} \underbrace{(\omega_2 x_1 + \omega_3 x_2) x_3 - b_3 x_3^2}_{g_s(x_1(t), x_2(t), x_3(t), \omega_2, \omega_3)} \\ \mathbf{0}_{3 \times 1} \end{bmatrix}, \end{cases} \quad (2.2)$$

where

$$w_s^\top(x_1, x_2) = \begin{bmatrix} b_1 - b_3 x_1 & x_2 & 1 + x_1^2 & x_1 x_2 \\ b_2 - b_3 x_2 & -x_1 & x_1 x_2 & 1 + x_2^2 \end{bmatrix}. \quad (2.3)$$

The system (2.2) exhibits the structure of the general non-linear system to which IBO may be applied. To apply the IBO, the following assumptions are in order:

ASSUMPTION 2.1

1. Let $\mathbf{x}(t) = [x_1(t), x_2(t), x_3(t), \boldsymbol{\theta}^\top]^\top$ be bounded: $\|\mathbf{x}(t)\| < M$, $M > 0$ for every $t \geq 0$. Let $\Omega = \{\mathbf{x}(t) \in \mathbb{R}^6 : \|\mathbf{x}(t)\| < M\}$. Further, for some fixed constant $\gamma > 1$, let $\Omega_\gamma = \{\mathbf{x}(t) \in \mathbb{R}^6 : \|\mathbf{x}(t)\| < \gamma M\}$.
2. Let $v_i(\tau)$ denote the i th column of $w_s^\top(x_1(t), x_2(t))$ in (2.3). There are no non-trivial constants κ_i (for $i = 1, 2, 3, 4$) such that

$$\sum_{i=1}^4 \kappa_i v_i(\tau) = 0, \quad (2.4)$$

for all $\tau \in [t, t + \mu]$, where $\mu > 0$ is a sufficiently small constant.

It is worth mentioning that the observability condition of IBO is stated in an integral form (page 65 of Jankovic & Ghosh, 1995). In the following, we show that Assumption 2.1 satisfies the IBO observability condition. From Assumption 2.1, there do not exist constants κ_i (for $i = 1, \dots, 4$) with $\sum_{i=1}^4 \kappa_i^2 \neq 0$ such that $\sum_{i=1}^4 \kappa_i v_i(t) = 0$. Therefore, for any non-zero 4×1 vector v with $\|v\| = 1$, we have $v^\top w_s(x_1, x_2) w_s^\top(x_1, x_2) v > \varepsilon \|v\|^2 = \varepsilon$. Therefore, $w_s(x_1, x_2) w_s^\top(x_1, x_2) > \varepsilon \mathbb{I}$ and the IBO observability condition is satisfied. Estimation of $x_3(t)$, along with the unknown motion parameters $\boldsymbol{\theta}$, can thus be obtained via direct application of the IBO. The specific form of the observer when applying the IBO to the system in (2.2) is given below.

Let

$$\hat{\boldsymbol{\theta}}(t) = [\hat{\omega}_1(t), \hat{\omega}_2(t), \hat{\omega}_3(t)]^\top. \quad (2.5)$$

The following observer can be designed for the system (2.2):

$$\left\{ \begin{array}{l} \begin{bmatrix} \dot{\hat{x}}_1(t) \\ \dot{\hat{x}}_2(t) \end{bmatrix} = G A_m \begin{bmatrix} \hat{x}_1(t) - x_1(t) \\ \hat{x}_2(t) - x_2(t) \end{bmatrix} + w_s^\top(x_1, x_2) \begin{bmatrix} \hat{x}_3(t) \\ \hat{\theta}(t) \end{bmatrix}, \\ \begin{bmatrix} \dot{\hat{x}}_3(t) \\ \dot{\hat{\theta}}(t) \end{bmatrix} = -G^2 w_s(x_1(t), x_2(t)) P \begin{bmatrix} \hat{x}_1(t) - x_1(t) \\ \hat{x}_2(t) - x_2(t) \end{bmatrix} \\ \quad + \begin{bmatrix} g_s(x_1(t), x_2(t), \hat{x}_3(t), \hat{\omega}_2(t), \hat{\omega}_3(t)) \\ \mathbf{0}_{3 \times 1} \end{bmatrix}, \\ \hat{\mathbf{x}}(t_i^+) = M \frac{\hat{\mathbf{x}}(t_i^-)}{\|\hat{\mathbf{x}}(t_i^-)\|}, \end{array} \right. \quad (2.6)$$

where $\hat{\mathbf{x}}(t) = [\hat{x}_1(t), \hat{x}_2(t), \hat{x}_3(t), \hat{\theta}(t)^\top]^\top$ denotes the estimate of $\mathbf{x}(t)$, G is a scalar constant and A_m is a 2×2 Hurwitz matrix. The matrix P is the positive-definite solution of the Lyapunov equation $A_m^\top P + P A_m = -Q$, where Q is a positive-definite symmetric matrix. The sequence t_i is defined as follows:

$$t_i = \min\{t: t > t_{i-1} \text{ and } \|\hat{\mathbf{x}}(t)\| \geq \gamma M\}, t_0 = 0, \quad (2.7)$$

where γ is a fixed constant. According to Theorem 2.3 in Jankovic & Ghosh (1995, p. 65), there exists a positive constant G_0 such that choosing $G > G_0$ ensures the estimation errors $[\hat{x}_1(t) - x_1(t), \hat{x}_2(t) - x_2(t), \hat{x}_3(t) - x_3(t), \hat{\theta}^\top(t) - \theta^\top]^\top$ converge to zero exponentially.

3. Fast estimator

In vision-based applications, continuous extraction of the target's information is often unavailable due to environmental factors, limited field of view of the camera or failure in the image processing module. Fast estimation becomes important in these situations when the target loss cannot be avoided. In this section, range identification in the presence of unknown motion parameters is pursued using a recently-developed fast estimator. Preliminary results of the fast estimator were presented in Ma (2007b). Detailed proofs and derivations are provided here. The analysis of the fast estimator is further extended to characterize the performance of the fast estimator with respect to non-zero initialization error. The fast estimator enables estimation of the unknown time-varying parameters in the system dynamics via large update gain and a low-pass filter.

If the time-varying unknown signal is linearly parameterized in unknown constant parameters, the fast estimator can be further augmented by a RLS algorithm to estimate the unknown constant parameters. Under certain PE-type conditions, the RLS algorithm ensures the convergence of parameter estimation. Details of the RLS algorithm and the PE condition are reviewed in Appendix C.

3.1 Problem formulation

This section presents details of the fast estimator. Consider the following system dynamics:

$$\dot{x}(t) = A_m x(t) + \omega(t), \quad x(0) = x_0, \quad (3.1)$$

where $x(t) \in \mathbb{R}^n$ is the system state vector, $\omega(t) \in \mathbb{R}^n$ is a vector of unknown time-varying signals or parameters and A_m is a known $n \times n$ Hurwitz matrix. Let

$$\omega(t) \in \Omega, \quad (3.2)$$

where Ω is a known compact set. There exists a positive constant μ_ω such that

$$\|\omega(t)\| \leq \mu_\omega < \infty, \quad \forall t \geq 0. \quad (3.3a)$$

The signal $\omega(t)$ is further assumed to be continuously differentiable with uniformly bounded derivative:

$$\|\dot{\omega}(t)\| \leq d_\omega < \infty, \quad \forall t \geq 0, \quad (3.3b)$$

where d_ω is a positive constant. The estimation objective is to design a fast estimator that provides fast estimation of $\omega(t)$.

3.2 Fast estimator

The proposed fast estimator consists of a state predictor, an update law, and a low-pass filter that extracts the estimation information.

We consider the following state predictor:

$$\dot{\hat{x}}(t) = A_m \hat{x}(t) + \hat{\omega}(t), \quad \hat{x}(0) = x_0, \quad (3.4)$$

which has the same structure as the system in (3.1). The only difference is that the unknown parameters $\omega(t)$ are replaced by their estimates $\hat{\omega}(t)$ that are governed by the following update law:

$$\dot{\hat{\omega}}(t) = \Gamma_c \text{Proj}(\hat{\omega}(t), -P\tilde{x}(t)), \quad \hat{\omega}(0) = \hat{\omega}_0, \quad (3.5)$$

where $\tilde{x}(t) = \hat{x}(t) - x(t)$ is the error signal between the state of the system and the state predictor, $\Gamma_c \in \mathbb{R}^+$ is the update gain, chosen sufficiently large, and P is the solution of the algebraic equation $A_m^\top P + P A_m = -Q$, $Q > 0$. Definition of the projection operator is given in the Appendix.

The estimate of the unknown signal is generated by

$$\omega_e(s) = C(s)\hat{\omega}(s), \quad \omega_e(0) = \hat{\omega}_0, \quad (3.6)$$

where $C(s)$ is a diagonal matrix with its i th diagonal element $C_i(s)$ being a strictly proper stable transfer function with low-pass gain $C_i(0) = 1$. One simple choice is

$$C_i(s) = \frac{c}{s + c}. \quad (3.7)$$

3.3 Convergence results

The main result of the fast estimator in Section 3 is that it ensures $\omega_e(t)$ estimates the unknown signal $\omega(t)$ with the final precision bound

$$\frac{\gamma_c}{\sqrt{\Gamma_c}} + \|1 - C(s)\|_{\mathcal{L}_1} \|\omega\|_{\mathcal{L}_\infty}, \quad (3.8)$$

where γ_c is to be given in (3.22a) and definition of the \mathcal{L}_∞ norm is reviewed in the Appendix. To quantify the above performance bound, an intermediate signal $\omega_r(t)$ is introduced as

$$\omega_r(s) = C(s)\omega(s), \quad \omega_r(0) = \hat{\omega}_0. \quad (3.9)$$

The precision bound in (3.8) is obtained through a triangulation of the performance bound of $(\omega_e(t) - \omega_r(t))$ and $(\omega_r(t) - \omega(t))$, respectively. The performance bound of $(\omega_e(t) - \omega_r(t))$ is first presented in Theorem 3.1, followed by that of $(\omega_r(t) - \omega(t))$ in (3.31). To quantify the performance bound of $(\omega_e(t) - \omega_r(t))$, we need the following lemma.

LEMMA 3.1 Given the system in (3.1) and the fast estimator in (3.4–3.6), the tracking error between the system state and the predictor state is bounded as follows:

$$\|\tilde{x}\|_{\mathcal{L}_\infty} \leq \sqrt{\frac{\omega_m}{\lambda_{\min}(P)\Gamma_c}}, \quad (3.10)$$

where

$$\omega_m = 4\mu_\omega^2 + 4\mu_\omega d_\omega \frac{\lambda_{\max}(P)}{\lambda_{\min}(Q)}. \quad (3.11)$$

Proof. Consider the following candidate Lyapunov function:

$$V(\tilde{x}(t), \tilde{\omega}(t)) = \tilde{x}^\top(t)P\tilde{x}(t) + \tilde{\omega}^\top(t)\tilde{\omega}(t)/\Gamma_c, \quad (3.12)$$

where

$$\tilde{\omega}(t) \triangleq \hat{\omega}(t) - \omega(t). \quad (3.13)$$

It follows from (3.1) and (3.4) that

$$\dot{\tilde{x}}(t) = A_m\tilde{x}(t) + \tilde{\omega}(t), \quad \tilde{x}(0) = 0. \quad (3.14)$$

Using the projection-based update law from (3.5), we have the following upper bound for $\dot{V}(t)$:

$$\dot{V}(t) \leq -\tilde{x}^\top(t)Q\tilde{x}(t) + 2|\tilde{\omega}^\top(t)\dot{\omega}(t)/\Gamma_c|. \quad (3.15)$$

The projection algorithm ensures that $\hat{\omega}(t) \in \mathcal{Q}$ for all $t \geq 0$, and therefore

$$\max_{t \geq 0} (\tilde{\omega}^\top(t)\tilde{\omega}(t)/\Gamma_c) \leq 4\mu_\omega^2/\Gamma_c, \quad \forall t \geq 0. \quad (3.16)$$

If at any t

$$V(t) > \omega_m/\Gamma_c, \quad (3.17)$$

then it follows from equations (3.12), (3.16) and (3.17) that

$$\tilde{x}^\top(t)P\tilde{x}(t) > 4\mu_\omega d_\omega \frac{\lambda_{\max}(P)}{\Gamma_c \lambda_{\min}(Q)}. \quad (3.18)$$

Hence,

$$\tilde{x}^\top(t) Q \tilde{x}(t) > \frac{\lambda_{\min}(Q)}{\lambda_{\max}(P)} \tilde{x}^\top(t) P \tilde{x}(t) > 4\mu_\omega d_\omega / \Gamma_c.$$

The upper bounds in (3.3b) along with the projection-based update laws lead to the following upper bound:

$$\frac{\tilde{\omega}^\top(t) \dot{\omega}(t)}{\Gamma_c} \leq 2 \frac{\mu_\omega d_\omega}{\Gamma_c}. \quad (3.19)$$

Hence, if $V(t) > \frac{\omega_m}{\Gamma_c}$, it follows from equation (3.15) that

$$\dot{V}(t) < 0. \quad (3.20)$$

Since we have set $\hat{x}(0) = x(0)$, we can verify that

$$V(0) \leq 4\mu_\omega^2 / \Gamma_c < \omega_m / \Gamma_c,$$

and it follows from (3.20) that $V(t) \leq \frac{\omega_m}{\Gamma_c}$ for any $t \geq 0$. Since $\lambda_{\min}(P) \|\tilde{x}(t)\|^2 \leq \tilde{x}^\top(t) P \tilde{x}(t) \leq V(t)$, then

$$\|\tilde{x}(t)\|^2 \leq \frac{\omega_m}{\lambda_{\min}(P) \Gamma_c},$$

which concludes the proof. \square

The performance bound between $\omega_e(t)$ and $\omega_r(t)$ is quantified in the following theorem.

THEOREM 3.1 Given the system in (3.1) and the fast estimator in (3.4–3.6), we have

$$\|\omega_e - \omega_r\|_{\mathcal{L}_\infty} \leq \frac{\gamma_c}{\sqrt{\Gamma_c}}, \quad (3.21)$$

where

$$\gamma_c = \|C(s)H^{-1}(s)\|_{\mathcal{L}_1} \sqrt{\frac{\omega_m}{\lambda_{\min}(P)}}, \quad (3.22a)$$

$$H(s) = (s\mathbb{I} - A_m)^{-1}. \quad (3.22b)$$

Proof. From equations (3.1) and (3.4), we have

$$s x(s) - x_0 = A_m x(s) + \omega(s), \quad s \hat{x}(s) - x_0 = A_m \hat{x}(s) + \hat{\omega}(s),$$

which leads to

$$x(s) = H(s)[\omega(s) + x_0], \quad \hat{x}(s) = H(s)[\hat{\omega}(s) + x_0], \quad (3.23)$$

and hence

$$\tilde{x}(s) = \hat{x}(s) - x(s) = H(s)(\hat{\omega}(s) - \omega(s)), \quad (3.24)$$

where $\omega(s)$ and $\hat{\omega}(s)$ are the Laplace transformation of $\omega(t)$ and $\hat{\omega}(t)$, respectively. It follows from equations (3.6) and (3.9) that

$$\begin{aligned}\omega_e(s) - \omega_r(s) &= C(s)(\hat{\omega}(s) - \omega(s)) \\ &= C(s)H^{-1}(s)H(s)(\hat{\omega}(s) - \omega(s)) \\ &= C(s)H^{-1}(s)\tilde{x}(s).\end{aligned}\tag{3.25}$$

Since $C(s)H^{-1}(s)$ is a matrix of stable and proper transfer functions, its \mathcal{L}_1 -norm exists and is bounded. Hence, we have

$$\|\omega_e - \omega_r\|_{\mathcal{L}_\infty} \leq \|C(s)H^{-1}(s)\|_{\mathcal{L}_1} \|\tilde{x}\|_{\mathcal{L}_\infty}.\tag{3.26}$$

It follows from Lemma 3.1 that

$$\|\omega_e - \omega_r\|_{\mathcal{L}_\infty} \leq \|C(s)H(s)^{-1}\|_{\mathcal{L}_1} \sqrt{\frac{\omega_m}{\lambda_{\max}(P)\Gamma_c}},$$

which along with (3.22a) leads to (3.21). \square

COROLLARY 3.1 Given the system in (3.1) and the fast estimator in (3.4–3.6), we have

$$\lim_{\Gamma_c \rightarrow \infty} (\omega_e(t) - \omega_r(t)) = 0, \quad \forall t \geq 0.\tag{3.27}$$

We then characterize the performance bound between $\omega_r(t)$ and $\omega(t)$. For simplicity, we use a first-order $C(s)$ as given in (3.7). It follows from (3.9) that

$$\dot{\omega}_r(t) = -c\omega_r(t) + c\omega(t), \quad \omega_r(0) = \hat{\omega}_0.\tag{3.28}$$

We note that $\omega_r(t)$ can be decomposed into two components:

$$\omega_r(t) = \omega_{r_1}(t) + \omega_{r_2}(t),\tag{3.29}$$

where $\omega_{r_1}(t)$ and $\omega_{r_2}(t)$ are defined as follows:

$$\dot{\omega}_{r_1}(t) = -c\omega_{r_1}(t) + c\omega(t), \quad \omega_{r_1}(0) = \omega_0,\tag{3.30a}$$

$$\dot{\omega}_{r_2}(t) = -c\omega_{r_2}(t), \quad \omega_{r_2}(0) = \hat{\omega}_0 - \omega_0.\tag{3.30b}$$

It follows from (3.30a) that

$$\|\omega_{r_1} - \omega\|_{\mathcal{L}_\infty} = \|1 - C(s)\|_{\mathcal{L}_1} \|\omega\|_{\mathcal{L}_\infty}.\tag{3.31}$$

Since

$$\lim_{c \rightarrow \infty} \|1 - C(s)\|_{\mathcal{L}_1} = 0,\tag{3.32}$$

the norm $\|\omega_{r_1} - \omega\|_{\mathcal{L}_\infty}$ can be rendered arbitrarily small by increasing the bandwidth of $C(s)$. Further, $\omega_{r_2}(t)$ decays to zero exponentially and the settling time is inverse proportional to the bandwidth of $C(s)$. Increasing the bandwidth of $C(s)$ implies that $\omega_{r_2}(t)$ decays to zero faster. It can be observed from equations (3.21) and (3.31) that $\omega_e(t)$ estimates $\omega(t)$ with the final precision given in (3.8) when the transients of $C(s)$ due to the initial condition $-\omega_0$ die out.

REMARK 3.1 It was proved in Dippold (2009, Proposition 11, pp. 103–104) that if the Hurwitz matrix A_m in (3.1) is a diagonal matrix of the form $A_m = \text{diag}(a_{m_1}, a_{m_2})$ where a_{m_1} and a_{m_2} are negative constants, then for the choice of $C(s)$ in (3.7),

$$\begin{aligned} \|C(s)H^{-1}(s)\|_{\mathcal{L}_1} &= \left\| \frac{c}{s+c} (s\mathbb{I} - A_m)^{-1} \right\|_{\mathcal{L}_1} \\ &= \frac{1}{\min\{|a_{m_1}|, |a_{m_2}|\}}. \end{aligned} \quad (3.33)$$

It follows from equations (3.21) and (3.33) that

$$\|\omega_e - \omega_r\|_{\mathcal{L}_\infty} \leq \frac{1}{\Gamma_c \min\{|a_{m_1}|, |a_{m_2}|\}} \sqrt{\frac{\omega_m}{\lambda_{\min}(P)}}, \quad (3.34)$$

which is independent of c in (3.7). Thus, selection of the bandwidth of $C(s)$ and the update gain Γ_c is independent of each other. Increasing the update gain Γ_c renders the term $\|\omega_e - \omega_r\|_{\mathcal{L}_\infty}$ arbitrarily small. Note that increasing the update gain Γ_c requires faster computation and smaller integration step. Further, increasing the bandwidth of $C(s)$ ensures that $\omega_r(t)$ tracks $\omega(t)$ arbitrarily closely both in transient and steady state.

The low-pass filter removes the high-frequency component in its input signal. Though this is a well-adopted method, the proposed fast estimator that consists of the state predictor (3.4), the update law (3.5) and the application of the low-pass filter (3.6) is novel for the following features: (1) with the help of the low-pass filter, the proposed estimator is able to estimate the time-varying signal with a final precision bound that can be made arbitrarily small by increasing the update gain and the bandwidth of the low-pass filter, subject to hardware limit; (2) the proposed estimator estimates the unknown time-varying signal with specifically characterized final precision bound given in (3.8) and (3) all derivations are performed analytically.

3.4 Performance of fast estimation in the presence of non-zero initialization error

The performance of the fast estimator is also analysed with respect to non-zero initialization error $\hat{x}_0 - x_0$, associated with the following state predictor:

$$\dot{\hat{x}}(t) = A_m \hat{x}(t) + \hat{\omega}(t), \quad \hat{x}(0) = \hat{x}_0 \neq x_0. \quad (3.35)$$

LEMMA 3.2 Given the system in (3.1) and the fast estimator with the state predictor in (3.35), we have

$$\|\tilde{x}(t)\| \leq \kappa(t), \quad \forall t \geq 0, \quad (3.36)$$

where

$$\begin{cases} \kappa(t) = \sqrt{\frac{(V(0) - \omega_m/\Gamma_c)e^{-\alpha t} + \omega_m/\Gamma_c}{\lambda_{\min}(P)}}, \\ \alpha = \frac{\lambda_{\min}(Q)}{\lambda_{\max}(P)}, \end{cases} \quad (3.37)$$

and ω_m is given in (3.11).

Proof. The proof is similar to that performed for Lemma 3.1. The difference is to take care of the non-zero initialization error. Consider the same Lyapunov function in (3.12). Since $\hat{x}_0 \neq x_0$, equation (3.14) reduces to

$$\dot{\tilde{x}}(t) = A_m \tilde{x}(t) + \tilde{\omega}(t), \quad \tilde{x}(0) = \hat{x}_0 - x_0. \quad (3.38)$$

The projection algorithm ensures that equations (3.15) and (3.16) are true, along the trajectory $\tilde{x}(t)$ in (3.38). Thus,

$$\begin{aligned} V(t) &= \tilde{x}^\top(t) P \tilde{x}(t) + \tilde{\omega}^\top(t) \tilde{\omega}(t) / \Gamma_c \\ &\leq \tilde{x}^\top(t) P \tilde{x}(t) + 4\mu_\omega^2 / \Gamma_c \end{aligned} \quad (3.39)$$

and

$$\begin{aligned} \tilde{x}^\top(t) Q \tilde{x}(t) &> \frac{\lambda_{\min}(Q)}{\lambda_{\max}(P)} \tilde{x}^\top(t) P \tilde{x}(t) \\ &> \frac{\lambda_{\min}(Q)}{\lambda_{\max}(P)} (V(t) - 4\mu_\omega^2 / \Gamma_c). \end{aligned} \quad (3.40)$$

For the derivative of the Lyapunov function, we have

$$\begin{aligned} \dot{V}(t) &= -\tilde{x}^\top(t) Q \tilde{x}(t) + 2\tilde{\omega}^\top(t) \dot{\omega}(t) / \Gamma_c \\ &\leq -\frac{\lambda_{\min}(Q)}{\lambda_{\max}(P)} V(t) + \frac{\lambda_{\min}(Q)}{\lambda_{\max}(P)} 4\mu_\omega^2 / \Gamma_c + 4\mu_\omega d_\omega / \Gamma_c \\ &= -\frac{\lambda_{\min}(Q)}{\lambda_{\max}(P)} V(t) + \frac{\lambda_{\min}(Q)}{\lambda_{\max}(P)} \frac{\omega_m}{\Gamma_c}, \end{aligned} \quad (3.41)$$

where ω_m is given in (3.11). It follows from (3.41) that

$$V(t) \leq (V(0) - \omega_m / \Gamma_c) e^{-\alpha t} + \omega_m / \Gamma_c, \quad (3.42)$$

where α is defined in (3.37). Since $\lambda_{\min}(P) \|\tilde{x}(t)\|^2 \leq \tilde{x}^\top(t) P \tilde{x}(t) \leq V(t)$, then

$$\|\tilde{x}(t)\|^2 \leq \frac{(V(0) - \omega_m / \Gamma_c) e^{-\alpha t} + \omega_m / \Gamma_c}{\lambda_{\min}(P)}, \quad (3.43)$$

which concludes the proof. \square

Let $\tilde{x}_a(t)$ be a signal with its Laplace transformation

$$\tilde{x}_a(s) = H(s)(\hat{x}_0 - x_0), \quad (3.44)$$

where $H(s)$ is given in (3.22b). The next theorem characterizes the performance bound of $(\omega_e(t) - \omega_r(t))$.

THEOREM 3.2 Given the system in (3.1) and the fast estimator with the state predictor in (3.35), we have

$$\|\omega_e(t) - \omega_r(t)\|_\infty \leq \psi(t) * [\kappa(t) + \|\tilde{x}_a(t)\|], \quad (3.45)$$

where $*$ denotes the convolution operation and

$$\psi(t) = \max_{i=1, \dots, n} \sqrt{\sum_{j=1}^m h_{ij}^2(t)}, \quad (3.46)$$

where $h_{ij}(t)$ is the i th row and j th column of the impulse response of $C(s)H^{-1}(s)$.

Proof. The proof is similar to that performed for Theorem 3.1. The difference is to take care of the non-zero initialization error. From equations (3.1) and (3.35), we have

$$s x(s) - x_0 = A_m x(s) + \omega(s), \quad s \hat{x}(s) - \hat{x}_0 = A_m \hat{x}(s) + \hat{\omega}(s),$$

which leads to

$$x(s) = H(s)[\omega(s) + x_0], \quad \hat{x}(s) = H(s)[\hat{\omega}(s) + \hat{x}_0],$$

and hence

$$\tilde{x}(s) = H(s)[\hat{\omega}(s) - \omega(s)] + H(s)(\hat{x}_0 - x_0), \quad (3.47)$$

where $H(s)$ is given in (3.22b). Then $\omega_e(s) - \omega_r(s)$ becomes

$$\begin{aligned} \omega_e(s) - \omega_r(s) &= C(s)[\hat{\omega}(s) - \omega(s)] = C(s)H^{-1}(s)[\tilde{x}(s) - H(s)(\hat{x}_0 - x_0)] \\ &= C(s)H^{-1}(s)[\tilde{x}(s) - \tilde{x}_a(s)], \end{aligned} \quad (3.48)$$

where $\tilde{x}_a(s)$ is given in (3.44). Since

$$\|\tilde{x}(t) - \tilde{x}_a(t)\| \leq \|\tilde{x}(t)\| + \|\tilde{x}_a(t)\| \leq \kappa(t) + \|\tilde{x}_a(t)\|, \quad (3.49)$$

where $\|\tilde{x}(t)\| \leq \kappa(t)$ is already shown in Lemma 3.2, it follows from Lemma 11 in Cao & Hovakimyan (2008, p. 65) that

$$\|\omega_e(t) - \omega_r(t)\|_\infty \leq \psi(t) * [\kappa(t) + \|\tilde{x}_a(t)\|],$$

where $\kappa(t)$ and $\psi(t)$ are given in (3.37) and (3.46), respectively. This completes the proof. \square

REMARK 3.2 Notice that $\kappa(t)$ in (3.37) is an exponentially decaying signal with the ultimate bound $\sqrt{\omega_m / [\lambda_{\min}(P) \Gamma_c]}$ as given in Lemma 3.1. Besides, $\|\tilde{x}_a(t)\|$ exponentially decays to zero. Thus, $(\omega_e(t) - \omega_r(t))$ will decay exponentially with the ultimate bound stated in Theorem 3.1.

If the time-varying signal $\omega(t)$ can be linearly parameterized in unknown constant parameters and known non-linear functions, extraction of the unknown parameters can be achieved by the RLS algorithm under a PE-type of condition. The RLS algorithm is reviewed in the Appendix.

4. Range identification via fast estimation

Denote

$$\eta(t) = \begin{bmatrix} \eta_1(t) \\ \eta_2(t) \end{bmatrix} \quad (4.1)$$

and write the first equation in (2.2) as

$$\begin{bmatrix} \dot{x}_1(t) \\ \dot{x}_2(t) \end{bmatrix} = w_s^\top(x_1(t), x_2(t)) \begin{bmatrix} x_3(t) \\ \boldsymbol{\theta} \end{bmatrix} = \eta(t), \quad x(0) = x_0, \quad (4.2)$$

where $\boldsymbol{\theta}$ is defined in (2.1) and $w_s^\top(x_1(t), x_2(t))$ is given in (2.3). That is,

$$\begin{bmatrix} b_1 - b_3x_1 & x_2 & 1 + x_1^2 & x_1x_2 \\ b_2 - b_3x_2 & -x_1 & x_1x_2 & 1 + x_2^2 \end{bmatrix} \begin{bmatrix} x_3(t) \\ \boldsymbol{\theta} \end{bmatrix} = \eta(t). \quad (4.3)$$

Letting

$$\begin{aligned} N_1(t) &= b_1(t) - b_3(t)x_1(t), \\ N_2(t) &= b_2(t) - b_3(t)x_2(t), \end{aligned} \quad (4.4)$$

equation (4.3) can be rewritten as

$$N_2(t)\eta_1(t) - N_1(t)\eta_2(t) = \begin{bmatrix} N_2(t)x_2 + N_1(t)x_1 \\ N_2(t)(1 + x_1^2) - N_1(t)x_1x_2 \\ N_2(t)x_1x_2 - N_1(t)(1 + x_2^2) \end{bmatrix}^\top \boldsymbol{\theta}. \quad (4.5)$$

The RLS method can be used to estimate $\boldsymbol{\theta}$ according to (7.6), with $\omega(t)$ replaced by $N_2(t)\eta_1(t) - N_1(t)\eta_2(t)$. Once $\boldsymbol{\theta}$ is available, equation (4.3) becomes

$$\begin{bmatrix} b_1 - b_3x_1 \\ b_2 - b_3x_2 \end{bmatrix} x_3 = \begin{bmatrix} \eta_1(t) \\ \eta_2(t) \end{bmatrix} - \begin{bmatrix} x_2 & 1 + x_1^2 & x_1x_2 \\ -x_1 & x_1x_2 & 1 + x_2^2 \end{bmatrix} \boldsymbol{\theta}, \quad (4.6)$$

where $x_3(t)$ can be extracted using the pseudoinverse.

Using the fast estimator in (3.4–3.6), estimation of $\eta(t)$ in (4.2), denoted by $\eta_e(t)$, can be obtained via the following steps:

- State predictor:

$$\begin{bmatrix} \hat{x}_1(t) \\ \hat{x}_2(t) \end{bmatrix} = A_m \begin{bmatrix} \tilde{x}_1(t) \\ \tilde{x}_2(t) \end{bmatrix} + \hat{\eta}(t), \quad \hat{x}(0) = x_0, \quad (4.7)$$

where $\tilde{x}_i(t) = \hat{x}_i(t) - x_i(t)$, for $i = 1, 2$. The above state predictor, along with the system dynamics in (4.2), gives the error dynamics $\dot{\tilde{x}}(t) = A_m\tilde{x}(t) + \tilde{\eta}(t)$, $\tilde{x}(0) = 0$.

- Update law for the parameter:

$$\dot{\hat{\eta}}(t) = \Gamma_c \text{Proj} \left(\hat{\eta}(t), -P \begin{bmatrix} \tilde{x}_1(t) \\ \tilde{x}_2(t) \end{bmatrix} \right), \quad \hat{\eta}(0) = \hat{\eta}_0. \quad (4.8)$$

- Applying low-pass filter:

$$\eta_e(s) = C(s)\hat{\eta}(s), \quad C(s) = \frac{c}{s+c}, \quad \eta_e(0) = \hat{\eta}_0. \quad (4.9)$$

A flow chart of state and parameter estimation of a rigid-body motion using the fast estimator is illustrated in Fig. 2. In the first step to estimate $\eta(t)$, both the estimation precision and transient time can

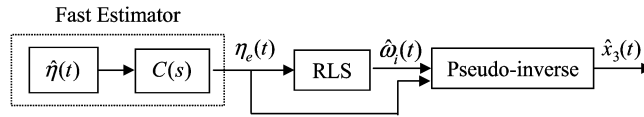


FIG. 2. Flow chart of applying the fast estimator for the range identification problem.

be arbitrarily reduced by increasing the bandwidth of $C(s)$ and larger Γ_c . In the second step of extracting parameters $\hat{\omega}_i(t)$ from $\eta_e(t)$ using the RLS method, fast speed can be achieved by properly tuning the RLS gains. Estimate of $x_3(t)$, denoted by $\hat{x}_3(t)$, can be obtained from $\eta_e(t)$ and $\hat{\omega}_i(t)$ via pseudoinverse.

5. Simulation results

State estimate of $[x_3(t), \theta^\top]^\top$ using the IBO in (2.6) and the fast estimator in (4.7–4.9) are implemented in Matlab, where the motion dynamics are

$$\begin{bmatrix} \dot{X}(t) \\ \dot{Y}(t) \\ \dot{Z}(t) \end{bmatrix} = \begin{bmatrix} 0 & -4 & -0.8 \\ 4 & 0 & -0.6 \\ 0.8 & 0.6 & 0 \end{bmatrix} \begin{bmatrix} X(t) \\ Y(t) \\ Z(t) \end{bmatrix} + \begin{bmatrix} 10 \\ 3\pi \sin(2\pi t) \\ 3\pi \sin(2\pi t + \pi/4) \end{bmatrix}, \quad (5.1)$$

with initial values

$$(X_0, Y_0, Z_0) = (1, 1.5, 2.5), \quad x_0 = (X_0/Z_0, Y_0/Z_0, 1/Z_0). \quad (5.2)$$

First, we present simulation results in the ideal case with no measurement noise. The design gains for the IBO and the fast estimator are chosen as

- IBO parameters (referring to (2.6)):

$$G = 10, \quad (\hat{x}_3(0), \hat{\omega}_1(0), \hat{\omega}_2(0), \hat{\omega}_3(0)) = (0, 0, 0, 0). \quad (5.3)$$

- Fast estimator parameters (referring to equations (7.6), (4.7), (4.8) and (4.9)):

$$p = 100, \quad \lambda = 0.99999, \quad \Gamma_c = 2 \times 10^4, \quad (\hat{\eta}_1(0), \hat{\eta}_2(0)) = (0, 0), \quad c = 100. \quad (5.4)$$

- Common parameters:

$$(\hat{x}_1(0), \hat{x}_2(0)) = (x_1(0), x_2(0)), \quad M = 20, \quad A_m = -\mathbb{I}_2, \quad P = 1/2 \times \mathbb{I}_2, \quad (5.5)$$

where \mathbb{I}_2 denotes the 2×2 identity matrix.

Estimate of ω_i (for $i = 1, 2, 3$) when using the IBO and the fast estimator is shown in Figs 3 and 4, respectively. Figure 4 (b) shows an enlarged view of Fig. 4 (a). State estimation error of $x_3(t)$ is plotted in Fig. 5 for comparison of these two methods. From Figs 3 and 4, it can be observed that the fast estimator achieves faster estimation of the motion parameters. The same is true for $x_3(t)$.

Simulation results are also presented in Figs 6–8 where 1% uniform noise is injected into the visual measurements via the Matlab function `randn()`. The simulation parameters are the same as above. In this case, when extracting $\hat{x}_3(t)$, the output from the pseudoinverse is further processed using a low-pass filter $\frac{30}{s+30}$ to give the final state estimation. We observe that corresponding plots with or without measurement noise are very similar.

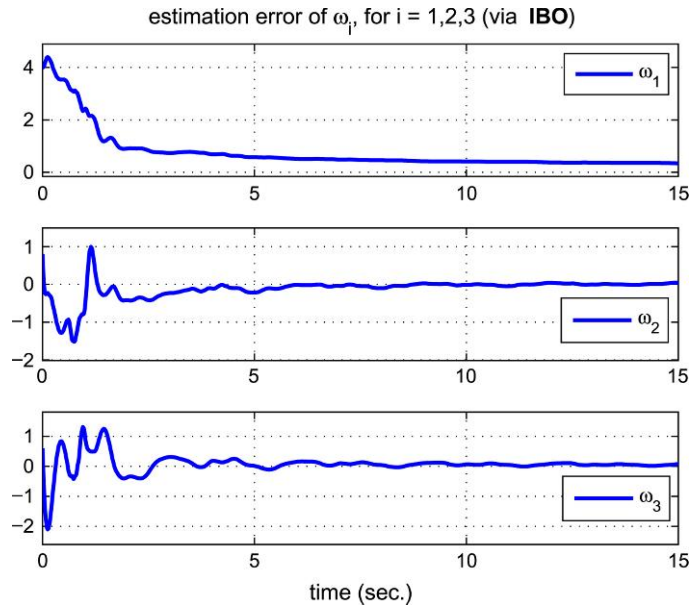


FIG. 3. Estimation of motion parameters via IBO (without measurement noise).

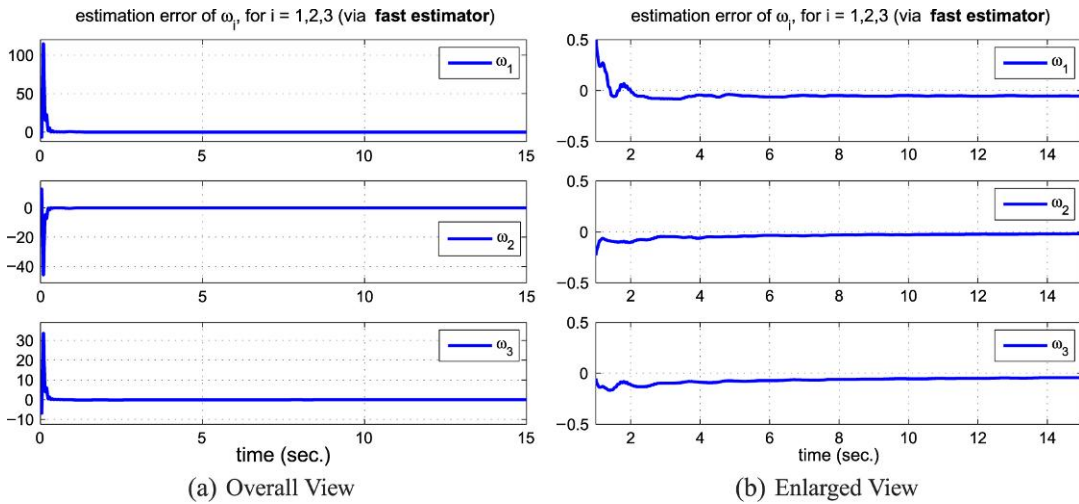


FIG. 4. Estimation of motion parameters via fast estimator (without measurement noise).

6. Further extension

In addition to the rigid-body motion in (1.1), extension to a more general motion, i.e. an affine motion, is discussed in this section.

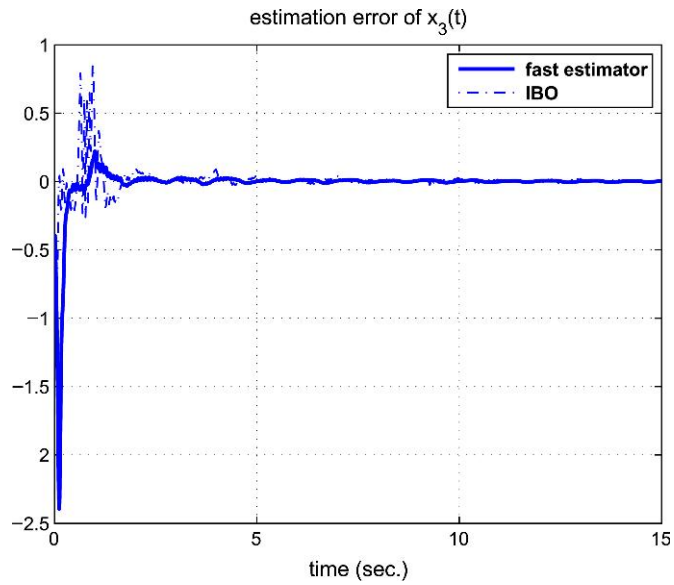


FIG. 5. Comparison of state estimation errors (without measurement noise).

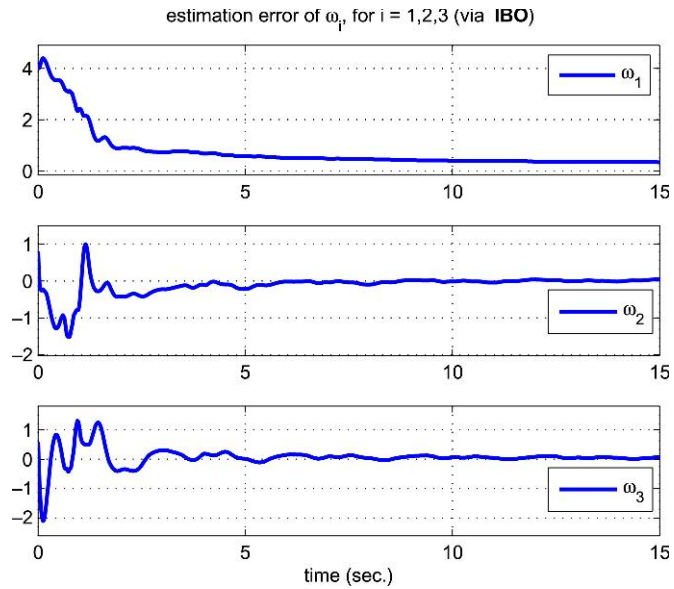


FIG. 6. Estimation of motion parameters via IBO (with measurement noise).

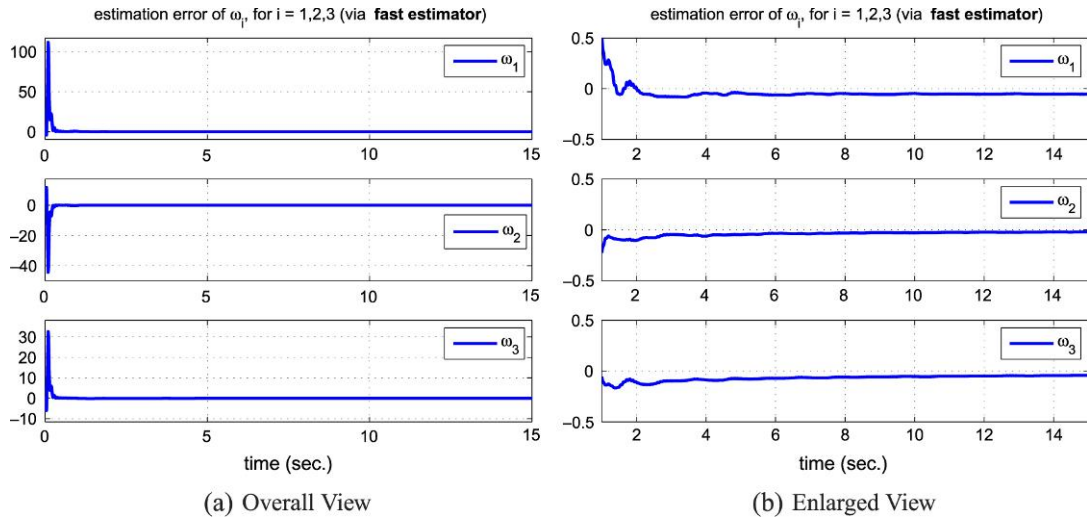


FIG. 7. Estimation of motion parameters via fast estimator (with measurement noise).

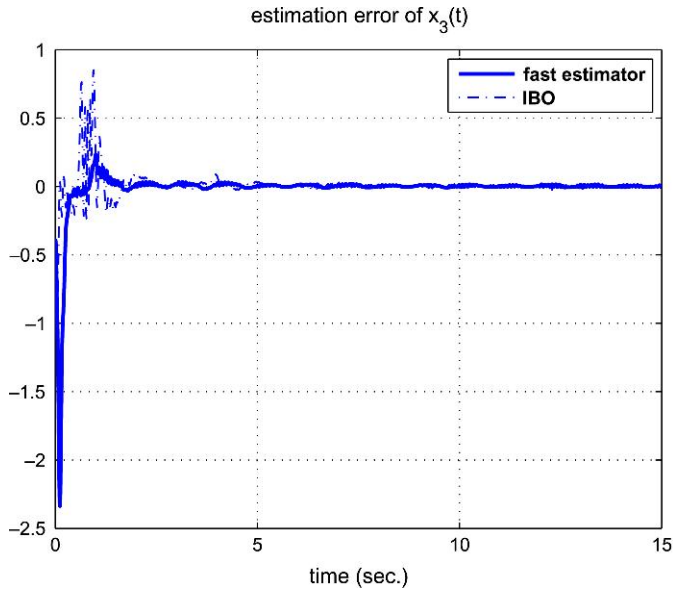


FIG. 8. Comparison of state estimation errors (with measurement noise).

6.1 Affine motion

For a general affine motion described by Dixon *et al.* (2003) and Ma *et al.* (2007a)

$$\begin{bmatrix} \dot{X}(t) \\ \dot{Y}(t) \\ \dot{Z}(t) \end{bmatrix} = \begin{bmatrix} a_{11} & a_{12} & a_{13} \\ a_{21} & a_{22} & a_{23} \\ a_{31} & a_{32} & a_{33} \end{bmatrix} \begin{bmatrix} X(t) \\ Y(t) \\ Z(t) \end{bmatrix} + \begin{bmatrix} b_1(t) \\ b_2(t) \\ b_3(t) \end{bmatrix}, \tag{6.1}$$

the rotational matrix contains nine parameters. Again, we limit the discussion to constant parameters a_{ij} . The system (6.1) with output observations (1.3) is equivalent to the following system Dixon *et al.* (2003) and Ma *et al.* (2007a):

$$\begin{cases} \begin{bmatrix} \dot{x}_1(t) \\ \dot{x}_2(t) \end{bmatrix} = \begin{bmatrix} b_1(t) - b_3(t)x_1(t) \\ b_2(t) - b_3(t)x_2(t) \end{bmatrix} \\ x_3(t) + \begin{bmatrix} a_{13} + (a_{11} - a_{33})x_1(t) + a_{12}x_2(t) - a_{31}x_1^2(t) - a_{32}x_1(t)x_2(t) \\ a_{23} + a_{21}x_1(t) + (a_{22} - a_{33})x_2(t) - a_{31}x_1(t)x_2(t) - a_{32}x_2^2(t) \end{bmatrix}, \\ \dot{x}_3(t) = -(a_{31}x_1(t) + a_{32}x_2(t) + a_{33})x_3(t) - b_3(t)x_3^2(t), \end{cases} \quad (6.2)$$

with the output given in (1.5).

Define

$$\vartheta = [a_{11}, a_{12}, a_{13}, a_{21}, a_{22}, a_{23}, a_{31}, a_{32}]^\top. \quad (6.3)$$

The system in (6.2) can be rewritten as

$$\begin{cases} \begin{bmatrix} \dot{x}_1(t) \\ \dot{x}_2(t) \end{bmatrix} = w_s^\top(x_1(t), x_2(t)) \begin{bmatrix} x_3(t) \\ \vartheta \end{bmatrix} - a_{33} \begin{bmatrix} x_1 \\ x_2 \end{bmatrix}, \\ \begin{bmatrix} \dot{x}_3(t) \\ \vartheta \end{bmatrix} = \begin{bmatrix} \underbrace{-(a_{31}x_1 + a_{32}x_2 + a_{33})x_3 - b_3x_3^2}_{g_s(x_1, x_2, x_3, a_{3j})} \\ \mathbf{0}_{8 \times 1} \end{bmatrix}, \end{cases} \quad (6.4)$$

where

$$w_s^\top(x_1, x_2) = \begin{bmatrix} b_1 - b_3x_1 & x_1 & x_2 & 1 & 0 & 0 & 0 & -x_1^2 & -x_1x_2 \\ b_2 - b_3x_2 & 0 & 0 & 0 & x_1 & x_2 & 1 & -x_1x_2 & -x_2^2 \end{bmatrix}. \quad (6.5)$$

Assuming that a_{ij} for $i, j = 1, 2, 3$ (except for a_{33}) are unknown constants, in the next we show how $x_3(t)$ and a_{ij} can be estimated using the fast estimator described in Section 3, followed by the RLS method. Note that a_{33} is assumed to be known.

REMARK 6.1 Assuming that the $[a_{ij}]$ (for $i, j = 1, 2, 3$) are unknown constants, the method described in Section 4 cannot lead to extraction of the nine unknown parameters in a straightforward way. Let $\theta_{9 \times 1}$ be a vector of these unknown constants as

$$\theta_{9 \times 1} = [a_{11}, a_{12}, a_{13}, a_{21}, a_{22}, a_{23}, a_{31}, a_{32}, a_{33}]^\top. \quad (6.6)$$

The system (6.2) can be written in the form of (2.2) with

$$w_s^\top(x_1, x_2) = \begin{bmatrix} b_1 - b_3x_1 & x_1 & x_2 & 1 & 0 & 0 & 0 & -x_1^2 & -x_1x_2 & -x_1 \\ b_2 - b_3x_2 & 0 & 0 & 0 & x_1 & x_2 & 1 & -x_1x_2 & -x_2^2 & -x_2 \end{bmatrix}. \quad (6.7)$$

The ten column vectors of $w_s^\top(x_1(t), x_2(t))$ in (6.7) are linearly dependent. For example, letting v_i denote the i th column of $w_s^\top(x_1, x_2)$, we have $v_{10} = -v_2 - v_6$. Thus, extraction of the nine unknown parameters cannot be performed by the RLS method since it violates the PE condition in (7.7). It is worth mentioning that the above restriction on the knowledge of a_{33} is not imposed by the method proposed in this paper. It is due to the nature of the estimation problem itself.

6.2 Fast estimation

Following the logic in Section 4, equation (4.2) becomes

$$\begin{bmatrix} \dot{x}_1(t) \\ \dot{x}_2(t) \end{bmatrix} = \underbrace{w_s^\top(x_1(t), x_2(t))}_{\eta(t)} \begin{bmatrix} x_3 \\ \boldsymbol{\vartheta} \end{bmatrix} - a_{33} \begin{bmatrix} x_1 \\ x_2 \end{bmatrix}, \tag{6.8}$$

where $\boldsymbol{\vartheta}$ and $w_s^\top(x_1(t), x_2(t))$ are given in (6.3) and (6.5), respectively. Equation (4.5) becomes

$$N_2(t)\eta_1(t) - N_1(t)\eta_2(t) = \underbrace{\begin{bmatrix} N_2(t) [x_1, x_2, 1]^\top \\ -N_1(t) [x_1, x_2, 1]^\top \\ (N_1(t)x_2 - N_2(t)x_1) [x_1, x_2]^\top \end{bmatrix}}_{\phi^\top(t)} \boldsymbol{\vartheta}, \tag{6.9}$$

for the same $N_1(t)$ and $N_2(t)$ in (4.4). The RLS method can be used to extract the unknown parameters $\boldsymbol{\vartheta}$ according to (7.6). Once $\boldsymbol{\vartheta}$ is available, we have

$$\begin{bmatrix} b_1 - b_3x_1 \\ b_2 - b_3x_2 \end{bmatrix} x_3(t) = \begin{bmatrix} \eta_1(t) \\ \eta_2(t) \end{bmatrix} - \begin{bmatrix} x_1 & x_2 & 1 & 0 & 0 & 0 & -x_1^2 & -x_1x_2 \\ 0 & 0 & 0 & x_1 & x_2 & 1 & -x_1x_2 & -x_2^2 \end{bmatrix} \boldsymbol{\vartheta}, \tag{6.10}$$

where $x_3(t)$ can be extracted using the pseudoinverse. Application of the fast estimator is similar to those performed in Section 4 and is omitted from here.

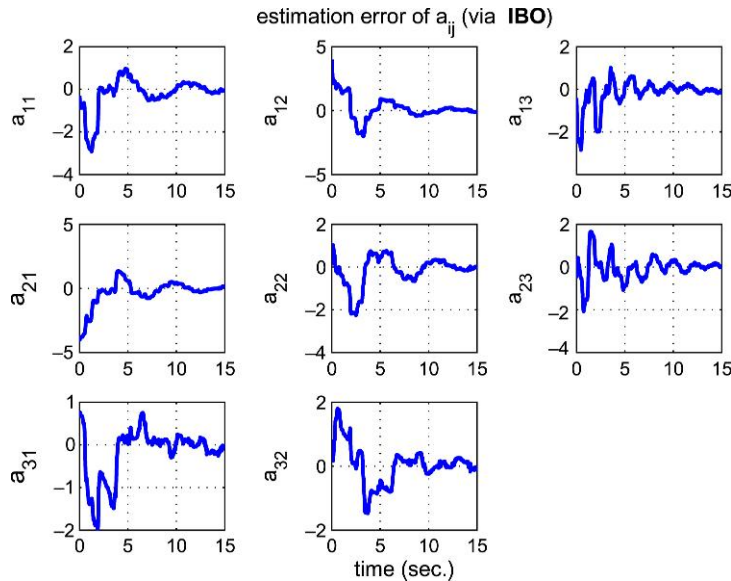


FIG. 9. Estimation of motion parameters via IBO (affine).

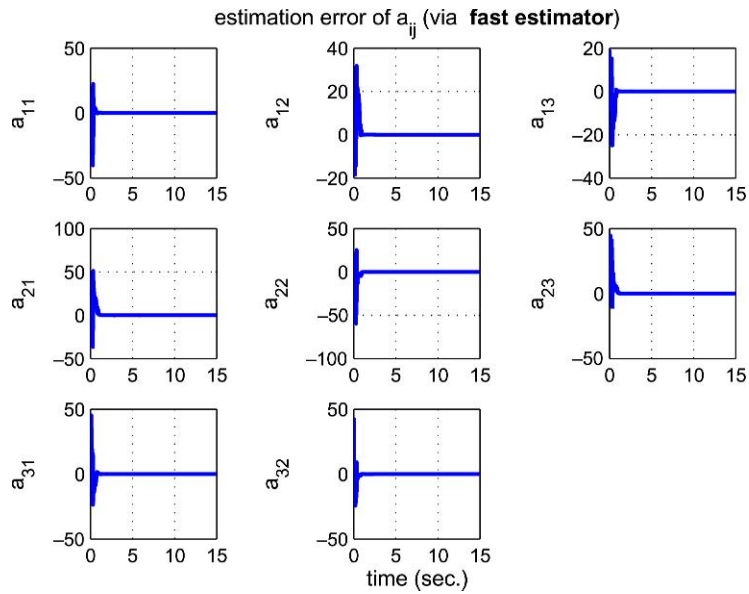


FIG. 10. Estimation of motion parameters via fast estimator (affine).

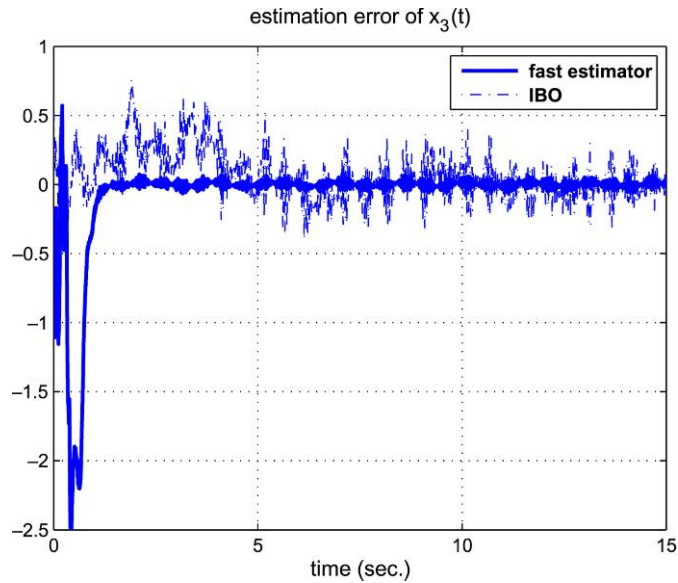


FIG. 11. Comparison of state estimation errors (affine).

6.3 Simulation results

Estimation of $[x_3(t), \boldsymbol{\theta}^\top]^\top$ using the IBO and the fast estimator are implemented in Matlab with the following motion dynamics:

$$\begin{bmatrix} \dot{X}(t) \\ \dot{Y}(t) \\ \dot{Z}(t) \end{bmatrix} = \begin{bmatrix} 0.3 & -4 & 0.4 \\ 4 & -0.2 & 0.4 \\ -0.7 & -0.5 & 0 \end{bmatrix} \begin{bmatrix} X \\ Y \\ Z \end{bmatrix} + \begin{bmatrix} 2\pi \sin(2\pi t) \\ 2\pi \cos(2\pi t) \\ 0 \end{bmatrix}, \quad (6.11)$$

for the same initial values in (5.2). The parameters are selected to be $G = 30$, $\Gamma_c = 2 \times 10^7$ and $c = 200$. Other parameters for the IBO and the fast estimator are the same as those in equations (5.3–5.5). Simulation results are presented in Figs 9–11 where the visual measurements are corrupted by 1% noise. It can be observed that the fast estimator achieves faster estimation of the motion parameters. The same is true for $x_3(t)$.

7. Conclusion

A fast estimator is proposed and applied to the range identification problem for both rigid-body and affine motions in the presence of unknown constant rotational parameters. The fast estimator allows for fast estimation of the unknown time-varying signal via large update gain and low-pass filter. Simulation results show that fast convergence speed is achieved compared to existing non-linear perspective observers. Future research will consider motion estimation with unknown rotational and translational parameters.

Funding

Army Research Office (#W911NF-06-1-0330); Office of Naval Research (#N00014-06-1-0801); Air Force Office of Scientific Research Multidisciplinary University Research Initiative subcontract (F49620-03-1-0401).

REFERENCES

- AZARBAYEJANI, A. & PENTLAND, A. (1995) Recursive estimation of motion, structure, and focal length. *IEEE Trans. Autom. Control*, **17**, 562–575.
- CAO, C. & HOVAKIMYAN, N. (2008) \mathcal{L}_1 adaptive controller for systems with unknown time-varying parameters and disturbances in the presence of nonzero trajectory initialization error. *Int. J. Control*, **81**, 1147–1161.
- CHEN, X. & KANO, H. (2002) A new state observer for perspective systems. *IEEE Trans. Autom. Control*, **47**, 658–663.
- CHEN, X. & KANO, H. (2004) State observer for a class of nonlinear systems and its application to machine vision. *IEEE Trans. Autom. Control*, **49**, 2085–2091.
- CHIUSO, A., FAVARO, P., JIN, H. & SOATTO, S. (2002) Structure from motion causally integrated over time. *IEEE Trans. Pattern Anal. Mach. Intell.*, **24**, 523–535.
- CHO, H., LEE, K. & LEE, S. (2001) A new robust 3D motion estimation under perspective projection. *IEEE Conference on Image Processing*, Thessaloniki, Greece, pp. 660–663.
- DAHL, O., NYBERG, F., HOLST, J. & HEYDEN, A. (2005) Linear design of a nonlinear observer for perspective systems. *IEEE Conference on Robotics and Automation*, Barcelona, Spain, pp. 429–435.
- DIAMANTARAS, K., PAPADIMITRION, T., STRINTZIS, M. & ROUMELIOTIS, M. (1998) Total least squares 3-D motion estimation. *IEEE Conference on Image Processing*, Chicago, IL, pp. 923–927.

- DIAMANTARAS, K. & STRINTZIS, M. (1996) Camera motion parameter recovery under perspective projection. *IEEE Conference on Image Processing*, Lausanne, Switzerland, pp. 807–810.
- DIPPOLD, A. (2009) Vision-based obstacle avoidance for multiple vehicles performing time-critical missions. *Ph.D Thesis*, Virginia Polytechnic Institute and State University, Blacksburg, VA.
- DIXON, W., FANG, Y., DAWSON, D. & FLYNN, T. (2003) Range identification for perspective vision systems. *IEEE Trans. Autom. Control*, **48**, 2232–2238.
- GHOSH, B., JANKOVIC, M. & WU, Y. (1994) Perspective problems in system theory and its application to machine vision. *J. Math. Syst. Estim. Control*, **4**, 3–38.
- GHOSH, B. & LOUCKS, E. (1995) A perspective theory for motion and shape estimation in machine vision. *SIAM J. Control Optim.*, **33**, 1530–1559.
- GHOSH, B. & MARTIN, C. (2002) Homogeneous dynamical systems theory. *IEEE Trans. Autom. Control*, **47**, 462–472.
- GUPTA, S., AIKEN, D., HU, G. & DIXON, W. (2006) Lyapunov-based range and motion identification for a nonaffine perspective dynamic system. *American Control Conference*, Minneapolis, MN, pp. 4471–4476.
- JANKOVIC, M. & GHOSH, B. (1995) Visually guided ranging from observations of points, lines and curves via an identifier based nonlinear observer. *Syst. Control Lett.*, **25**, 63–73.
- KANO, H., GHOSH, B. & KANAI, H. (2001) Single camera based motion and shape estimation using extended Kalman filtering. *Math. Comput. Model.*, **34**, 511–525.
- KARAGIANNIS, D. & ASTOLFI, A. (2005) A new solution to the problem of range identification in perspective vision systems. *IEEE Trans. Autom. Control*, **50**, 2074–2077.
- KHALIL, H. (2002) *Nonlinear Systems*. Englewood Cliffs, NJ: Prentice Hall.
- MA, L., CAO, C., HOVAKIMYAN, N., DIXON, W. & WOOLSEY, C. (2007a) Range identification in the presence of unknown motion parameters for perspective vision systems. *American Control Conference*, New York, pp. 972–977.
- MA, L., CAO, C., HOVAKIMYAN, N., WOOLSEY, C. & DIXON, W. (2007b) Fast estimation for range identification in the presence of unknown motion parameters. *International Conference on Informatics in Control, Automation and Robotics - Signal Processing, Systems Modeling and Control*, Angers, France, pp. 157–164.
- MA, L., CHEN, Y. & MOORE, K. (2005a) Perspective dynamic systems with 3D imaging surfaces. *American Control Conference*, Portland, OR, pp. 3671–3675.
- MA, L., CHEN, Y. & MOORE, K. (2005b) Range identification for perspective dynamic system with a single homogeneous observation. *Int. J. Appl. Math. Comput. Sci.*, **15**, 63–72.
- MATTHIES, L., KANADE, T. & SZELISKI, R. (1989) Kalman filter-based algorithms for estimating depth from image sequences. *Int. J. Comput. Vision*, **3**, 209–236.
- NARENDRA, K. & ANNASWAMY, A. (2005) *Stable Adaptive Systems*. Mineola: Dover Publications.
- PAPADIMITRIOU, T., DIAMANTARAS, K., STRINTZIS, M. & ROUMELIOTIS, M. (2000) Robust estimation of rigid-body 3-D motion parameters based on point correspondences. *IEEE Trans. Circuits Syst. Video Technol.*, **10**, 541–549.
- POMET, J. & PRALY, L. (1992) Adaptive nonlinear regulation: estimation from the Lyapunov equation. *IEEE Trans. Autom. Control*, **37**, 729–740.
- SOATTO, S., FREZZA, R., & PERONA, P. (1996) Motion estimation via dynamic vision. *IEEE Trans. Autom. Control*, **41**, 393–413.
- TAKAHASHI, S. & GHOSH, B. (2002) Motion and shape identification with vision and range. *IEEE Trans. Autom. Control*, **47**, 1392–1396.
- VERHAEGEN, M. (1989) Round-off error propagation in four generally-applicable, recursive, least-squares estimation schemes. *Automatica*, **25**, 437–444.
- WITTENMARK, K. (1995) *Adaptive Control*, 2nd edn. Addison-Wesley.
- ZHOU, K. & DOYLE, J. (1998) *Essentials of Robust Control*. Englewood Cliffs, New York, NJ: Prentice Hall.

Appendix A

We recall basic definitions and facts from linear systems theory (Khalil, 2002; Zhou & Doyle, 1998).

DEFINITION 7.1 For a signal $\zeta(t) = [\zeta_1(t) \cdots \zeta_n(t)]^T \in \mathbb{R}^n$ defined for all $t \geq 0$, the \mathcal{L}_∞ -norm is

$$\|\zeta\|_{\mathcal{L}_\infty} = \max_{i=1, \dots, n} (\sup_{\tau \geq 0} |\zeta_i(\tau)|).$$

DEFINITION 7.2 The \mathcal{L}_1 -norm of an asymptotically stable and proper single-input-single-output system is defined

$$\|H(s)\|_{\mathcal{L}_1} = \int_0^\infty |h(t)| dt,$$

where $h(t)$ is the impulse response of $H(s)$.

DEFINITION 7.3 For an asymptotically stable and proper m input n output system $H(s)$, the \mathcal{L}_1 -norm is defined as

$$\|H(s)\|_{\mathcal{L}_1} = \max_{i=1, \dots, n} \left(\sum_{j=1}^m \|H_{ij}(s)\|_{\mathcal{L}_1} \right),$$

where $H_{ij}(s)$ is the i th row and j th column entry of $H(s)$.

Appendix B

The projection operator is defined as Pomet & Praly (1992):

DEFINITION 7.4 Consider a convex compact set with a smooth boundary given by

$$\Omega_c \triangleq \{\theta \in \mathbb{R}^n \mid f(\theta) \leq c\}, \quad 0 \leq c \leq 1,$$

where $f: \mathbb{R}^n \rightarrow \mathbb{R}$ is the following smooth convex function:

$$f(\theta) = \frac{\theta^\top \theta - \theta_{\max}^2}{\epsilon_\theta \theta_{\max}^2}, \quad (7.1)$$

where θ_{\max} is the norm bound imposed on the parameter vector θ and ϵ_θ denotes the convergence tolerance of our choice. Let the true value of the parameter θ , denoted by θ^* , belong to Ω_0 , i.e. $\theta^* \in \Omega_0$. The projection operator is defined as

$$\text{Proj}(\theta, y) \triangleq \begin{cases} y & \text{if } f(\theta) < 0, \\ y & \text{if } f(\theta) \geq 0 \text{ and } \nabla f^\top y \leq 0, \\ y - \underbrace{\frac{\nabla f}{\|\nabla f\|}}_{\text{unit vector}} \underbrace{\left\langle \frac{\nabla f^\top}{\|\nabla f\|}, y \right\rangle}_{\text{projection}} \underbrace{f(\theta)}_{\text{scaling}} & \text{if } f(\theta) \geq 0 \text{ and } \nabla f^\top y > 0. \end{cases} \quad (7.2)$$

Appendix C

The RLS algorithm is reviewed here. Consider a linear scalar regression model

$$\omega_k = \theta^\top \phi_k + e_k, \quad (7.3)$$

where

$$\theta = [\theta_1, \theta_2, \dots, \theta_n]^\top \quad (7.4)$$

is the $n \times 1$ vector of the plant parameters, and

$$\phi_k = [\phi_{k,1}, \phi_{k,2}, \dots, \phi_{k,n}]^\top \quad (7.5)$$

is the $n \times 1$ regressor vector at time instant k , while e_k is a zero-mean discrete white noise sequence with variance σ_k^2 . When the observation of (ω_k, ϕ_k) has been obtained for $k = 1, \dots, N$ (with $N > n$), the RLS estimate for θ , denoted by $\hat{\theta}$, can be obtained in the following discrete form (Verhaegen, 1989):

$$\begin{cases} L_k = \frac{P_{k-1}\phi_k}{\lambda + \phi_k^\top P_{k-1}\phi_k}, \\ \hat{\theta}_k = \hat{\theta}_{k-1} + L_k(\omega_k - \phi_k^\top \hat{\theta}_{k-1}), \\ P_k = \frac{1}{\lambda} \left(P_{k-1} - \frac{P_{k-1}\phi_k\phi_k^\top P_{k-1}}{\lambda + \phi_k^\top P_{k-1}\phi_k} \right), \end{cases} \quad (7.6)$$

where $P_0 = p\mathbb{I}_{p \times p}$ and $\lambda \in (0, 1]$. Coefficients p and λ are the design gains. When ϕ_k is persistently exciting during the observation period, RLS algorithm ensures the convergence of $\hat{\theta}(t)$ to θ . The convergence rate of the RLS can be increased by choosing large λ . The PE condition of the regressor vector is defined as Verhaegen (1989).

DEFINITION 7.5 The regressor vector ϕ_k is persistently exciting over the observation interval $k_0 \leq k \leq k_N$ with an exponentially forgetting factor $\lambda \leq 1$, if the following condition is satisfied:

$$\rho_1 \mathbb{I} \leq \sum_{k=k_0}^{k_N} \phi_k \phi_k^\top \lambda^{k_N-k} \leq \rho_2 \mathbb{I}, \quad (7.7)$$

for some positive $\rho_1 > 0$ and $\rho_2 > 0$.